

**Detection of the urban expansion over agricultural land using LULC change detection techniques: case study El-Mahalla el-koubra City-Egypt****Eng. Mostafa MOSAAD \*****Dr. A.K. Helmy\*\*****Dr. Mahmoud Safwat\*****Dr. Fawzy Eltohamy\****\* Egyptian Armed Forces**\*\*National Authority of Remote Sensing and Space Sciences, Cairo, Egypt*

**ABSTRACT** *The increase in population density is one of the most important factors of urban expansion, which lead to a change in land use. To identify this change three tools are needed, they are Land use / land cover (LULC) change detection techniques, remote sensing data, and a computer system. This paper consists of two parts. The first part presents the concept, implementation, and assessment of seven LULC change detection techniques. These techniques are: post-classification, multi-date direct classification, image differencing, image rationing, image symmetric relative difference, change vector analysis (CVA), and principal component differencing (PCD). These techniques are implemented on remote sensing data of Sharm El-Sheikh city-Egypt, to detect the changes that took place over the period from 2000 to 2010. The post-classification change detection technique provided the highest accuracy of 95.2 %, while the principal component analysis differencing gave the lowest accuracy of 89.6 %. In the second part of the paper the post-classification change detection technique is implemented in the area of El-Mahalla El-cobra City-Egypt to detect the urban expansion over the agricultural area through the period from 2010 to 2015. The results showed that, the agricultural area was decreased by 6.04 % and the urban area was increased by 31.2 %.*

**Keywords** *Land use / Land cover (LULC), post classification, multi-date direct classification, image differencing, image rationing, image symmetric relative difference, Change Vector Analysis (CVA) and principal component differencing (PCD).*

## 1. Introduction

The earth's surface is changing due to human activity or natural phenomena, for example, urban growth, wildfires, agricultural expansion, storms, and military conflicts[1,2]. The earth's surface changes can be classified into two main categories: land use and land cover (LULC)[3]. Land cover is used to illustrate the physical state of the land surface such as cropland, forests, wetlands, human structures such as pavements, buildings and other aspects of the natural environment, including surface water, biodiversity, groundwater and soil type[4]. Land use illustrates the human way in using the land and its resources, including mining, agriculture, grazing, urban development and logging[5]. SO, Land use is considered to be a product of interactions between a society's cultural background, state and its physical needs on the one hand and the natural potential of land on the other hand[6]. LULC change detection techniques are considered to be the scientific and rapid way to detect the changes on the earth's surface, especially in the presence of the past and present land use/cover data of the study area[7]. environmental changes[6]. Generally, LULC are interdependent and closely related so they are often used interchangeably[8].

## 2. Categories of change detection methods

Change detection is the process of identifying differences in the state of an object or phenomenon by observing it at different times[9]. This observation can be done through remote sensing data of the study area acquired at different dates, where the changes in radiance values of the data appear as a result of land

cover changes. Since launching of the first Landsat satellite in 1972, till now, a wide range of remote sensing data with different spectral, spatial, radiometric and temporal resolutions are available[10]. This is necessary for the LULC change detection process[7]. It allows to perform LULC change detection on different temporal scales[11], and leads to the development and evaluation of many digital change detection methods for analyzing and detecting LULC changes[12]. It is extremely difficult to state the most proper method of detecting changes, generally it is application dependent. Generally change detection methods can be classified into two main categories: pre-classification and post-classification change detection methods [3]. Post-classification approach for change detection has been proven to be the most popular approach in change detection analysis[13]. This approach is based on rectification of more than one classified image, then comparison between them as shown in Fig (1). It minimizes sensor, atmospheric, and environmental differences because data from two dates are separately classified, thereby minimizing the problem of normalizing for atmospheric and sensor differences between two dates and it provides a complete matrix of land cover change when using multiple images[14]. The pre-classification comparison approach for change detection is identified as the most accurate change detection approach because, they are straight forward, effective for identifying and locating change and are easy to implement[15]. However, three aspects are critical for pre-classification techniques: selecting suitable thresholds to identify the changed areas, being sensitive to misregistration of pixels, and they cannot provide details of the nature of change or provide a matrix of information change[16]. Fig (2) illustrates the procedures of post-classification technique.

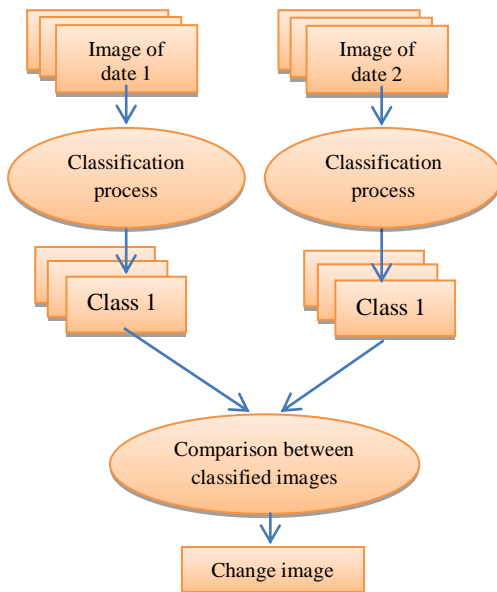


Fig (1): Main procedures of post-classification change detection approach

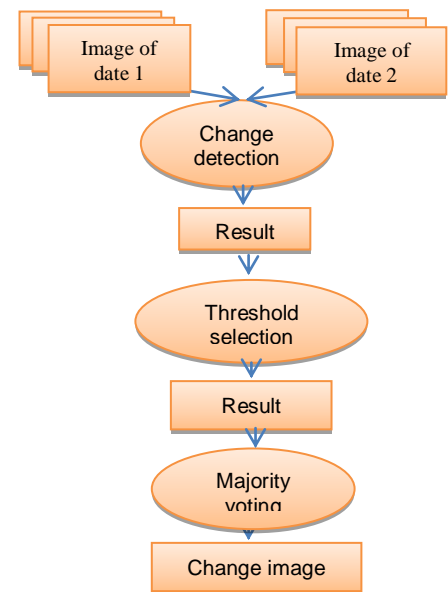


Fig (2): Main procedures of pre-classification change detection approach

### 3. The concepts of the selected change detection methods

Seven LULC change detection techniques are selected to be implemented on our dataset. These techniques are post-classification, direct multi-date classification (DMDC), image differencing (ID), image rationing (IR), image symmetric relative difference (ISRD), change vector analysis (CVA), and principal component differencing (PCD).

**ID** is based on the subtraction of two spatially registered imageries, pixel by pixel, as follows:

$$ID = X_i(t_2) - X_i(t_1) \quad (1)$$

Where X represents the multispectral images with I (number of bands) acquired at two different times  $t_1$  and  $t_2$ .

The pixels of changed area are expected to be distributed in the two tails of the histogram of the resultant image, and the unchanged area is grouped around zero. This simple method easily interprets the resultant image; however, it is crucial to properly define the thresholds to detect the change from non-change areas[3].

**IR** is similar to image differencing (ID) method. The only difference between them is the replacement of the differencing images by rationed images[3].

$$IR = X_i(t_2) / X_i(t_1) \quad (2)$$

**ISRD** is based on the use of symmetric relative difference formula to measure change[17], as follows:

$$ISRD = \frac{X_i(t_2) - X_i(t_1)}{X_i(t_2)} + \frac{X_i(t_2) - X_i(t_1)}{X_i(t_1)} \quad (3)$$

Dividing the difference by the pixel's value at time 1 and time 2 allows the derivation of a change image that measures the percentage change in the pixel, regardless of which image is chosen to be the initial image. For example a pixel that had a value of 20 at time 1 and a value of 80 at time 2 would have an absolute difference of 60, and a percentage change value in the change image of 375%:

$$[(80 - 20) / 20 + (80-20)/80] * 100 = 375\%$$

Another pixel with a value of 140 at time 1 and 200 at time 2 would also have an absolute difference of 60, but its percentage change would only be 72.86%:

$$[(200 - 140) / 140 + (200-140)/200] * 100 = 72.86\%$$

In most cases it can be assumed that the percentage change of a pixel's brightness value is more indicative of actual change in the image than simply the absolute difference[18].

**CVA** generates two outputs: a change vector image and a magnitude image. The spectral change vector explains the direction and magnitude of change from the first to the second date. The total change extent per pixel is calculated by determining the Euclidean distance between end points through dimensional change space, as follows:

$$|CVA(X(t_2), X(t_1))| = \sqrt{\sum_i (X_i(t_2) - X_i(t_1))^2} \quad (4)$$

A decision on change is made based on whether the change magnitude exceeds a specific threshold. The geometric concept of CVA is applicable to any number of spectral bands[19].

**PCD** is often as accepted as an effective transforms to derive information and compress dimensions. Most of the information is focused on the first two components. Particularly, the first component has the most information. The difference of the first principle component of two dates has the potential to

improve the change detection results, i.e.

$$PCD = PC1(X(t2)) - PC1(X(t1)) \quad (5)$$

The change detection is implemented based on threshold[3].

**DMDC** it combines the two images ( $X(t2)$  and  $X(t1)$ ) into a single image on which a classification is performed. The areas of changes are expected to present different statistics (i. e., distinct classes) compared to the areas with no changes[20].

**Post Classification** is based on the classification of the two images ( $X(t2)$  and  $X(t1)$ ) separately and then compared. Ideally, similar thematic classes are produced for each classification. Changes between the two dates can be visualized using a change matrix indicating, for both dates, the number of pixels in each class. This matrix allows us to interpret what changes occurred for a specific class. The main advantage of this method is the minimal impacts of radiometric and geometric differences between multi-date images. However, the accuracy of the final result is the product of accuracies of the two independent classifications (e.g., 64% final accuracy for two 80% independent classification accuracies)[20].

#### 4. Experimental work (part 1)

##### 4.1 Dataset of the study area

Fig (3) shows the dataset of Sharm el-Sheikh city- Egypt. It consists of two images acquired by Landsat 7 at 2000 and 2010 respectively. Each one represents an area that lies between Lat. 28 0 37.0091 N, Lon. 34 17 56.3381 E and Lat. 27 57 20.8804 N, Lon. 34 24 43.6080 E. Table (1) summarizes the characteristic of this dataset.

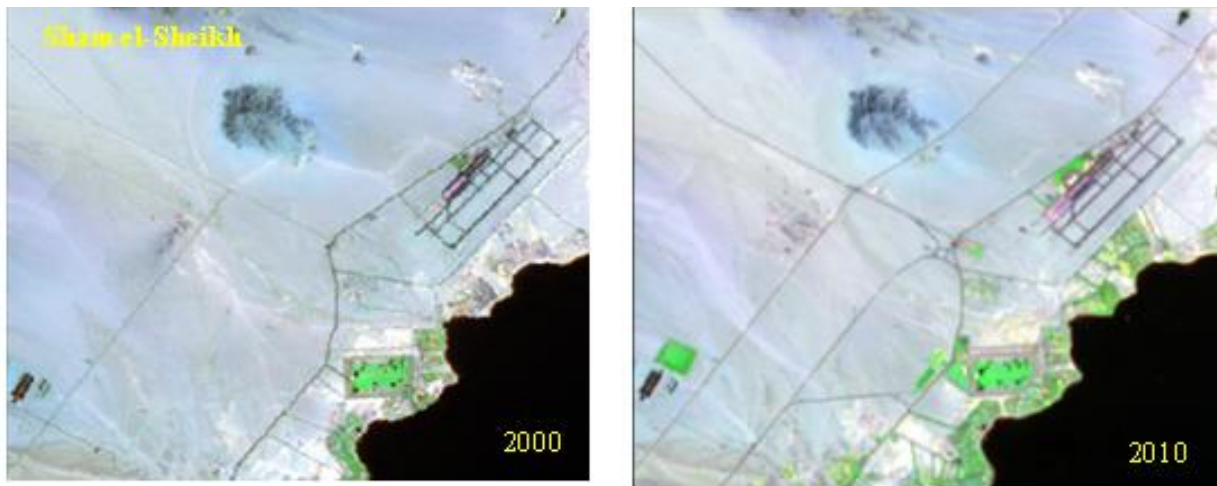


Fig (3): Dataset of Sharm el-Sheikh city- Egypt (Landsat 7)

Table (1): Characteristic of Sham el-Sheikh dataset

No	Spatial resolution	Radiometric resolution	Number of bands	Acquisition date	Size [pixels]		Area [km <sup>2</sup> ]
					Width	Height	
1	30 m	8 bits	3	2000	382	364	12.5143
2	30 m	8 bits	3	2010	382	364	12.5143

## 4.2 Computer system

A laptop machine with processor Intel(R)core(TM)i7-4500U CPU @1.80 GH 2.40 GH and RAM 8 GB is used. The model maker in the ERDAS IMAGINE 2014 software is used.

## 4.3 Experimental procedures

### 4.3.1 Pre-processing

Before implementation of the change detection techniques, it is essential that the changes in the objects of interest should indicate changes in radiance values not the changes produced from other factors such as variation of solar illumination conditions, atmospheric conditions, differences in soil moisture, viewing geometry at different acquisition times and acquiring from different sensor [14],[21],[22]. The impact of these factors may be reduced by selecting the appropriate data [9] and applying preprocessing treatment (image registration, if needed, and radiometric correction) [23]. In this paper the selected dataset had already registered. Radiometric correction is carried out to minimize the false change detection [24], so the pixel of the unchanged areas in one date, should take the same or close gray level values of the corresponding pixels in the other date. Histogram matching technique between the two images was applied for radiometric correction after normalization of both images[25].

### 4.3.2 Implementation and accuracy assessment of the change detection methods

The steps of implementation of each method are given in table (2). The change error matrix or the confusion matrix, table (5) is used to calculate the overall accuracy[26],[27]. It contains the reference information which was taken visually by comparing the dataset. The overall accuracy, user accuracy and the procedures, accuracy can be calculated from the change error matrix.

$$\text{The overall accuracy} = \frac{\text{total number of the correct classified change}}{\text{total number of classification}} \quad (6)$$

$$\text{The user accuracy} = \frac{\text{number in diagonal cells of the error matrix}}{\text{total number in row}} \quad (7)$$

$$\text{The procedure accuracy} = \frac{\text{number in diagonal cells of the error matrix}}{\text{total number in columns}} \quad (8)$$

The seven techniques were implemented by the model maker in the ERDAS IMAGINE 2014 software for dataset of **Sharm el-Sheikh** to provide an overview and assessment for LULC change detection techniques by using 250 random points to generate the change error matrix to evaluate the overall accuracy. Table (3) illustrates the overall accuracy and the rate of change in the area for each technique. Fig (4) shows the change image of the seven techniques.

Table (2): Steps of the seven change detection techniques implementation

Method	Procedures
Image differencing <b>ID</b>	<ol style="list-style-type: none"> <li>1- Applying Eqn (1)</li> <li>2- Threshold values were determined according to the statistical calculation by taking <math>(1 * STD)</math> to identify the land cover change. This step provides a binary image for each band, 1 as change and 0 as non-change.</li> <li>3- The change image is produced according to the majority voting between the binary images.</li> <li>4- The overall accuracy is calculated by Producing change error matrix using 250 random variables.</li> </ol>
Image rationing <b>IR</b>	<ol style="list-style-type: none"> <li>1- Apply Eqn (2)</li> <li>2- Thresholds were determined as mentioned before</li> <li>3- Change image is produced through majority voting between the binary images</li> <li>4- The overall accuracy is calculated by Producing change error matrix using 250 random variables</li> </ol>
Image symmetric Relative Difference <b>ISRD</b>	<ol style="list-style-type: none"> <li>1-Apply Eqn (3)</li> <li>2- Thresholds were determined as mentioned before</li> <li>3- Change image is produced through majority voting between the binary images</li> <li>4- The overall accuracy is calculated by Producing change error matrix using 250 random variables</li> </ol>
Change Vector analysis <b>CVA</b>	<ol style="list-style-type: none"> <li>1- Apply Eqn (4) to get the Euclidian distance between the two dates</li> <li>2- Thresholds were determined as mentioned before</li> <li>3- Change image is produced through majority voting between the binary images</li> <li>4- The overall accuracy is calculated by Producing change error matrix using 250 random variables</li> </ol>
Principal component differencing <b>PCD</b>	<ol style="list-style-type: none"> <li>1- Get the principle component of the two images</li> <li>2- Apply Eqn (5)</li> <li>3- Thresholds were determined as mentioned before</li> <li>4- Change image is produced through majority voting between the binary images</li> <li>5- The overall accuracy is calculated by Producing change error matrix using 250 random variables</li> </ol>
Direct multi-date classification <b>DMDC</b>	<ol style="list-style-type: none"> <li>1- First, stack all layers in date 1 and date 2 together</li> <li>2- Provide unsupervised classification using K-means classifier for the output image to get 20 classes</li> <li>3- Reduce the 20 classes to 2 classes using recode process to get the change image</li> <li>4- The overall accuracy is calculated by Producing change error matrix using 250 random variables</li> </ol>
Post classification	<ol style="list-style-type: none"> <li>1- Provide unsupervised classification using K-means classifier for each image to get 20 classes</li> <li>2- Reduce the 20 classes to 4 classes using recode process</li> <li>3- Compare the class pixel between the two images to produce the change image.</li> <li>4- The overall accuracy is calculated by Producing change error matrix using 250 random variables</li> </ol>



Table (3): Overall accuracy and the rate of change in area for each technique

Method	ID	IR	ISRD	CVA	PCD	DMDC	Post Classification
Overall Accuracy	92.4%	91.6 %	91.6 %	92.4 %	89.6 %	94.4 %	95.2 %
Rate of area Change	12.05%	11.13%	8.01 %	7.67%	19.43%	8.013%	11.21%

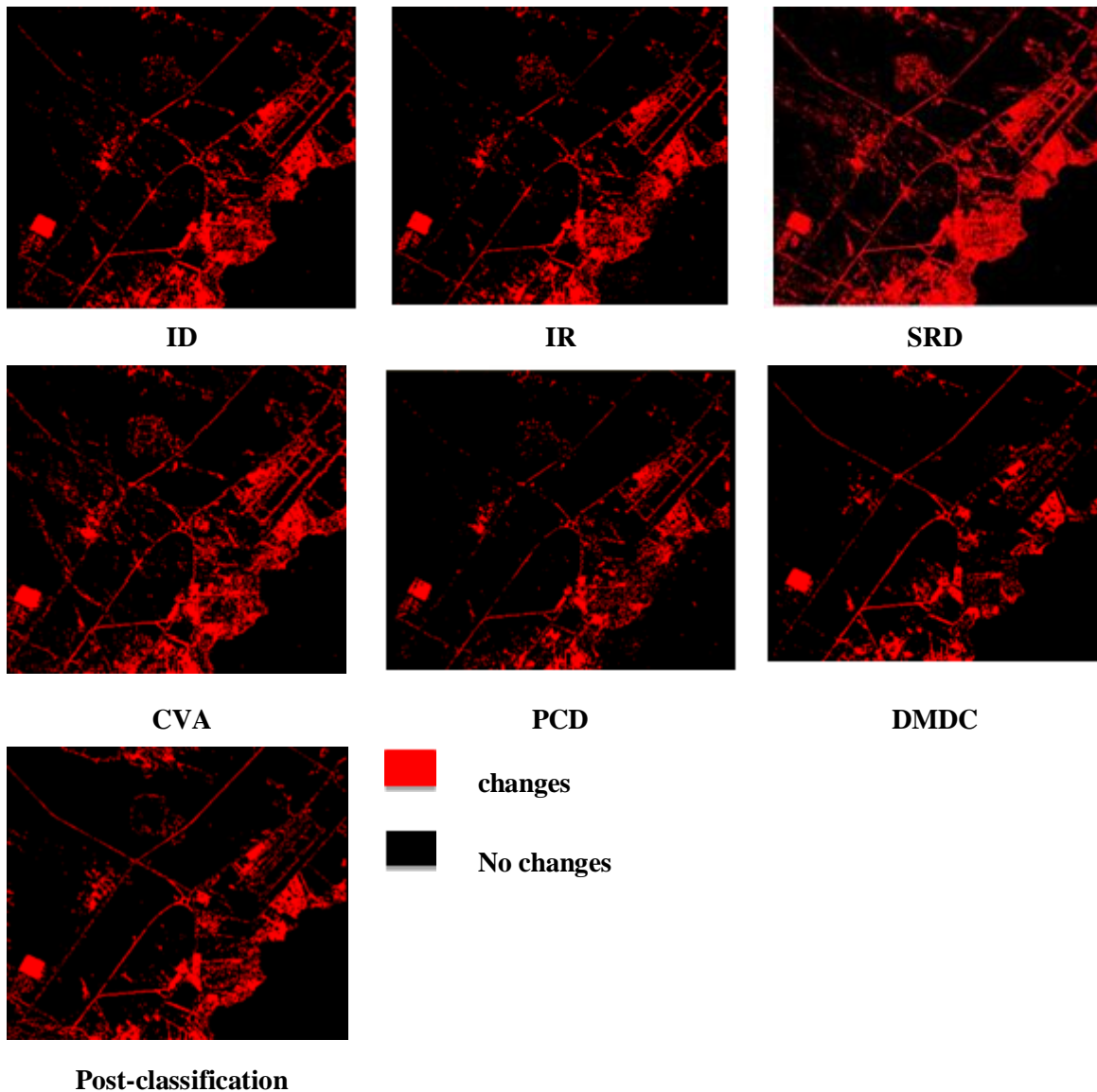


Fig (4): Change images after applying the seven techniques on Sharm el-Sheikh city- Egypt dataset

## 5. Experimental work (Part 2)

### 5.1 Dataset of the study area

Fig (5) shows the dataset of a village next neighbour of Mahalla al-Kubra city in Egypt. It consists of two images taken by El-Shayal Smart web on Line Software that could acquire Satellite images from Google Earth. The dataset was acquired at scale 1.600 Km. It lies between Lat. 30 57 46.9032 N, Lon. 31 14 35.4776 E and Lat. 30 54 47.00 N, Lon. 31 18 19.98. Table (4) summarizes the characteristic of this dataset.



Fig (5): dataset of Mahalla al-kubra city- Egypt ( Google Earth)

Table (4): characteristic of Mahalla al-Kubra cities Egypt dataset

No	Spatial resolution	Radiometric resolution	Number of bands	Acquisition date	Size [pixels]		Area [km <sup>2</sup> ]
					Width	Height	
1	6 m	8 bits	3	2010	1056	1007	38.2821
2	6 m	8 bits	3	2015	1056	1007	38.2821

**Note:** the same computer system is used with the second experimental work. Also the same pre-processing is applied to the dataset of the experimental work (part 2).

### 5.2 Implementation and accuracy assessment of post classification change detection method

The post classification technique was applied to the dataset, fig (5) to detect the urban expansion on agricultural land. 100 random points were selected to generate the change error matrix as shown in table (5). The overall accuracy of the change image 95 % and the procedure accuracy were 100 % and the user accuracy was 54.55%. The change image is given in Fig (6).

Table (5): the change error matrix of the change image that produced from the post classification techniques

Classified data	Reference data		
	No Change	Change	Total
No Change	89	0	89
Change	5	6	11
Total	94	6	100



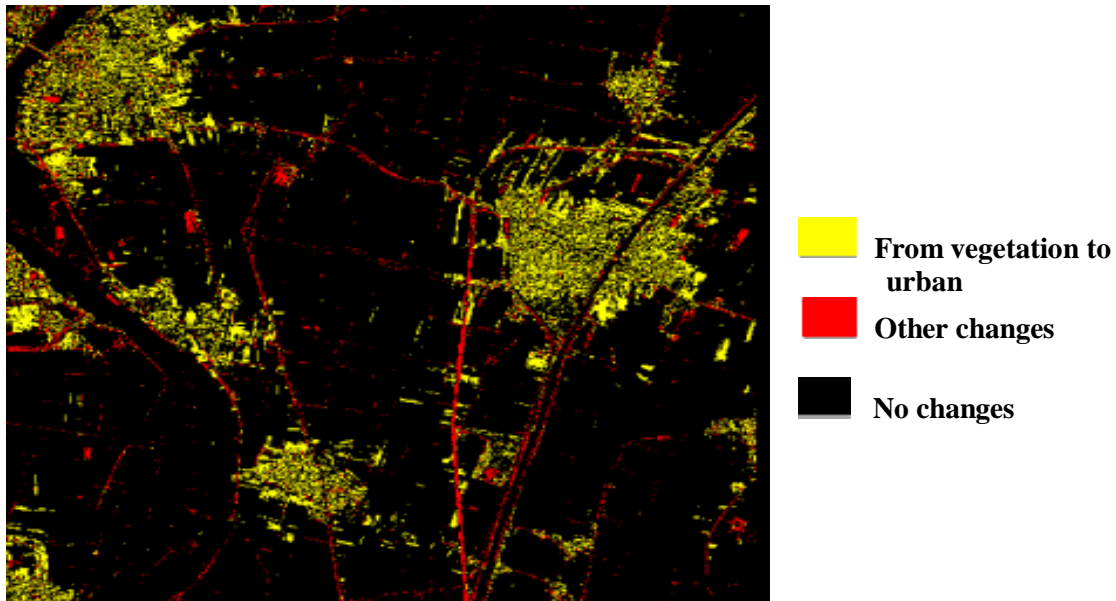


**Fig (6):** change image after applying the post classification technique for giving dataset of Mahalla al-Kubra city- Egypt

## 6. Analysis

Fig (7) gives a chart of the overall accuracy of the seven LULC change detection techniques that applied on the Sharm el-Sheik city. The post classification technique provides the highest overall accuracy compared to the other six techniques as it reduces the false change by minimizing sensor, atmospheric, and environmental differences. It has the ability of providing a complete matrix of land cover change, but there is one shortcoming of this method is the high requirements for a reasonable classification of categories as, the accuracy of the final result is the product of accuracies of the two independent classifications. Direct multi-date classification is quick and easy. It has the same advantages of the post-classification technique. In addition, the error rate will not be cumulative like post classification, but the results are difficult to interpret without a good knowledge of the study area. The change vector analysis has ability to process any number of spectral bands and also provides detailed information about change measure. Although the ISRD has lower accuracy than ID but its output has an indication of the actual change that happen in the study area. The principal component differencing technique is an effective transforms to derive information and compress dimensions. But, it provided the least overall accuracy as most of the information is focused on the first two components.

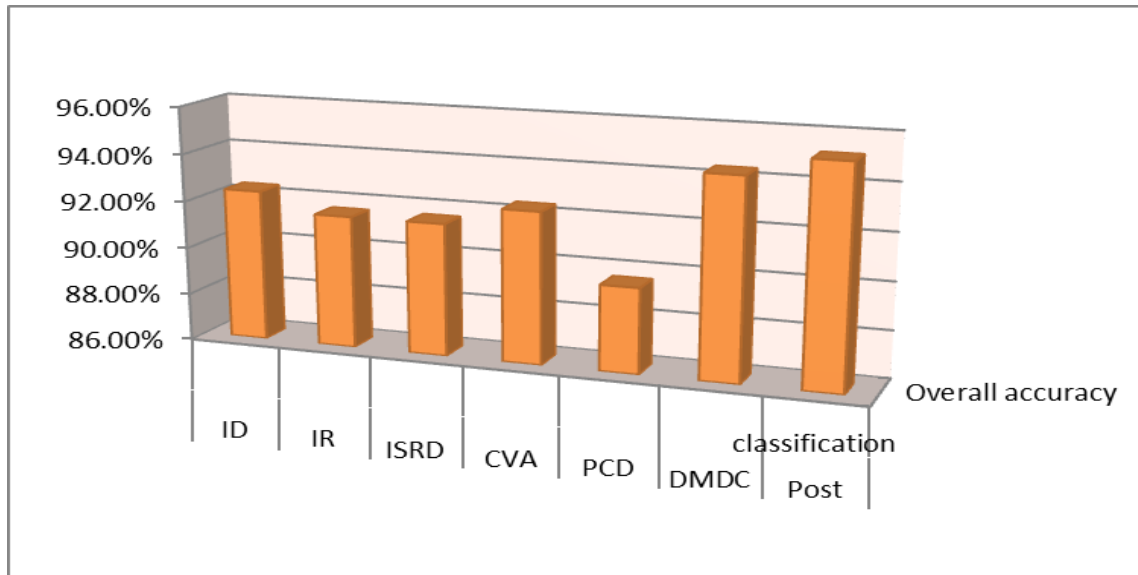


Fig (7):Chart of the overall accuracy of the seven change detection techniques that applied on the Sham el-Sheik city

Applying post classification techniques in the dataset of fig (5) indicated that 10.33 % has been changed from the total study area, the agricultural land was decreased by 6.04 % from the total agricultural area. The urban area was increased by 31.2 % from the urban area through the period from 2010 to 2015, as shown in Fig (8) and table (6).

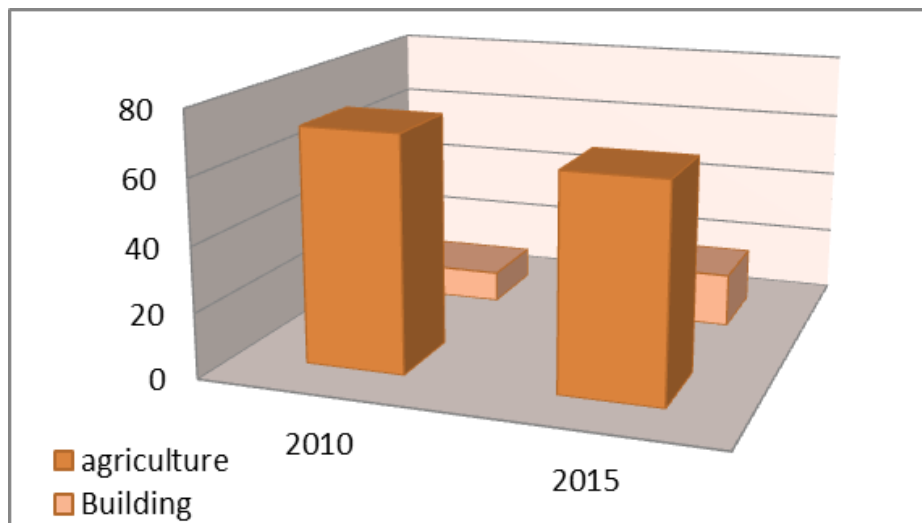


Fig (8):The changes that took place in the agriculture land through the period from 2010 to 2015 in El-Mahalla el-koubra city - Egypt

**Table (6):** The rate of change in area for agriculture and building that took place in El-Mahalla el-koubra city - Egypt

Type	2010	Percentage of total area	2015	Percentage of total area	Rate of change
Agriculture	27.6702 Km <sup>2</sup>	72.27 %	25.9967 Km <sup>2</sup>	65.28 %	Decreased by 6.04 %
Building	3.62344 Km <sup>2</sup>	9.46 %	5.27261 Km <sup>2</sup>	16.46 %	Increased by 31.2 %

## 7. Conclusion

Land Use and Land Cover change detection are one of the most important applications of remote sensing. Detecting and analyzing these changes can be done through a process commonly called 'change detection' by using remote sensing satellite data. There are many digital change detection techniques have been developed to detect and analyze Land Use and Land cover changes. They can be divided generally into two categories: pre-classification and post-classification change detection techniques. There are six main steps to detect the changes, determine the nature of the change detection problem, selection of remotely sensed data, image preprocessing, image processing or classification, selection of change detection techniques and finally evaluate the change detection results. However, the post-classification change detection technique in this study has provided the highest overall accuracy compared to the other six change detection techniques. But it is very difficult to assess the most proper technique for detecting Land Use and Land Cover changes in a particular area under study as the nature of the physical characteristics of the features of interest, the analyst skills and the characteristic of the available dataset vary.

## 8. References

1. Borak, J., E. Lambin, and A. Strahler, The use of temporal metrics for land cover change detection at coarse spatial scales. *International Journal of Remote Sensing*, 2000. 21(6-7): p. 1415-1432.
2. Agarwal, C., et al., A review and assessment of land-use change models: dynamics of space, time, and human choice. 2002.
3. Al-doski, J., S.B. Mansor, and H.Z.M. Shafri, Change Detection Process and Techniques. *Civil and Environmental Research*, 2013. 3(10): p. 37-45.
4. Jaiswal, R.K., R. Saxena, and S. Mukherjee, Application of remote sensing technology for land use/land cover change analysis. *Journal of the Indian Society of Remote Sensing*, 1999. 27(2): p. 123-128.
5. Ram, B. and A. Kolarkar, Remote sensing application in monitoring land-use changes in arid Rajasthan. *International Journal of Remote Sensing*, 1993. 14(17): p. 3191-3200.
6. Rawat, J., V. Biswas, and M. Kumar, Changes in land use/cover using geospatial techniques: A case study of Ramnagar town area, district Nainital, Uttarakhand, India. *The Egyptian Journal of Remote Sensing and Space Science*, 2013. 16(1): p. 111-117.
7. Chaurasia, R., et al., Land use change analysis for agricultural management—A case study of Tehsil Talwandi Sabo, Punjab. *Journal of the Indian Society of Remote Sensing*, 1996. 24(2): p. 115-123.
8. Verburg, P.H., et al., From land cover change to land function dynamics: a major challenge to improve land characterization. *Journal of environmental management*, 2009. 90(3): p. 1327-1335.
9. Singh, A., Review article digital change detection techniques using remotely-sensed data. *International Journal of Remote Sensing*, 1989. 10(6): p. 989-1003.

10. Williams, D.L., S. Goward, and T. Arvidson, Landsat. Photogrammetric Engineering & Remote Sensing, 2006. 72(10): p. 1171-1178.
11. Gibson, P.J., et al., Introductory remote sensing: digital image processing and applications. Vol. 11. 2000: Routledge London.
12. Dewidar, K.M., Detection of land use/land cover changes for the northern part of the Nile delta (Burullus region), Egypt. International Journal of Remote Sensing, 2004. 25(20): p. 4079-4089.
13. Foody, G.M., Status of land cover classification accuracy assessment. Remote sensing of environment, 2002. 80(1): p. 185-201.
14. Jensen, J.R., Introductory digital image processing 3rd edition, 2005, Upper Saddle River: Prentice Hall.
15. Sunar, F., An analysis of changes in a multi-date dataset: a case study in the Ikitelli area, Istanbul, Turkey. International Journal of Remote Sensing, 1998. 19(2): p. 225-235.
16. Lu, D., et al., Change detection techniques. International Journal of Remote Sensing, 2004. 25(12): p. 2365-2401.
17. Ehlers, M., D. Tomowski, and S. Klonus, Comparison of Automated Change Detection Methods.
18. Erdas , User guide Imagine Delta Cue . 2009. Norcross.
19. Chen, J., et al., Land-use/land-cover change detection using improved change-vector analysis. Photogrammetric Engineering & Remote Sensing, 2003. 69(4): p. 369-379.
20. Théau, J., Change detection, in Springer Handbook of Geographic Information 2012, Springer. p. 75-94.
21. Deer, P. Digital change detection techniques: Civilian and military applications. in International Symposium on Spectral Sensing Research. 1995.
22. Afify, H.A., Evaluation of change detection techniques for monitoring land-cover changes: A case study in new Burg El-Arab area. Alexandria Engineering Journal, 2011. 50(2): p. 187-195.
23. Jianya, G., et al., A review of multi-temporal remote sensing data change detection algorithms. The International Archives of the Photogrammetry, Remote Sensing and Spatial Information Sciences, 2008. 37(B7): p. 757-762.
24. Paolini, L., et al., Radiometric correction effects in Landsat multi-date/multi-sensor change detection studies. International Journal of Remote Sensing, 2006. 27(4): p. 685-704.
25. Richards J.A., J., Remotesensing Digital Image Analysis: An Introduction, 1999, Berlin: springer.
26. Rossiter, D., Statistical methods for accuracy assessment of classified thematic maps. Technical Note. Enschede: International Institute for Geo-information Science & Earth Observation (ITC), 2004.
27. Macleod, R.D. and R.G. Congalton, A quantitative comparison of change-detection algorithms for monitoring eelgrass from remotely sensed data. Photogrammetric Engineering and Remote Sensing, 1998. 64(3): p. 207-216.